Available online at www.eccomasproceedia.org
Eccomas Proceedia SMART (2023) 238-249

ECCOMAS
Proceedia

X ECCOMAS Thematic Conference on Smart Structures and Materials
SMART 2023
D.A. Saravanos, A. Benjeddou, N. Chrysochoidis and T. Theodosiou (Eds)

EXPERIMENTAL IDENTIFICATION OF ELECTROMECHANICAL COUPLING MATRICES FOR ACTIVE VIBRATION CONTROL

PRABAKARAN BALASUBRAMANIAN[*], GIOVANNI FERRARI[†], CELIA HAMEURY[†], TARCISIO M. P. SILVA[*], ABDULAZIZ BUABDULLA[*], GIULIO FRANCHINI [*] AND MARCO AMABILI [†*]

[*] Advanced Materials Research Center,
Technology Innovation Institute,
PO 9639,
Abu Dhabi, UAE

[†] McGill University,
Montreal, Canada

Abstract. PPF (Positive Position Feedback) is a highly effective algorithm for controlling mechanical vibrations in thin-walled structures. It is easy to use with piezoelectric patches and has useful modal characteristics. However, when using a MIMO (Multi-Input Multi-Output) architecture, it is necessary to convert physical signals from piezoelectric transducers into modal coordinates, which is done by placing participation matrices between sensors, controllers, and actuators. These matrices can be difficult to determine, especially when the number of actuators does not match the number of modes being controlled. Typically, an electromechanical FE (Finite Element) model or reduced-order model is used to estimate the participation matrices. This study proposes a method for estimating participation matrices using only experimental measurements. The method is tested on a two-dimensional composite plate with free edges, which has eight vibration modes. The plate's vibrations are controlled using four sensors and four actuators in a non-collocated configuration. The experimental identification of the electromechanical coupling allows for the simulation of uncontrolled and controlled vibrations of the plate when it is subjected to external disturbance. The resulting PPF AVC (Active Vibration Control) significantly reduces the vibration amplitude of all eight modes in laboratory experiments, with minimal impact on the following normal modes. The vibration reduction is verified at various points on the plate's surface when it is subjected to pseudo-random excitation. The proposed experimental identification technique greatly simplifies the design of PPF controls and makes AVC techniques more widely accessible by eliminating the need for electromechanical modeling.

Key words: Particle Swarm Optimization; active vibration control; non-collocated control; PPF; plate.

Peer-review under responsibility of the organizing committee of SMART 2023.
doi: 10.7712/150123.9781.441174

1 INTRODUCTION

Thin shells and plates are used in engineering due to their high stiffness and low weight. However, they are prone to large-amplitude vibrations which need to be mitigated [1]. Passive methods are not very effective and active and semi-active control methods are becoming more popular. Active Vibration Control (AVC) is one such method that requires the supply of external energy to counteract unwanted vibrations. Piezoelectric patches are commonly used for AVC due to their thinness, light weight, and ability to function as both sensors and actuators. They can even be used on gossamer membranes. Designs like Macro Fiber Composites (MFCs) have increased the force performance of piezoelectric patches. However, the practical application of AVC remains limited due to the complexity of the control algorithms, risk of instability, and the need for an external power supply.

AVC strategies are divided into feedforward and feedback strategies. Feedforward AVC is fast and cannot cause instability but requires detailed knowledge of the structure under test and the external disturbance causing unwanted vibrations. Feedforward has been effectively applied, such as the Filtered-x Least Mean Square (fxLMS) algorithm [2], [3] for Active Noise Cancellation (ANC) in acoustic applications [4]. Feedback control is simpler in principle but can cause dangerous instabilities. AVC systems can be characterized by the dimension and number of their active elements. Distributed piezoelectric elements have been proposed in the literature, but concentrated active elements, much smaller than the structures under test, are more prevalent due to simpler and more economic design [5]–[7].

This paragraph discusses the concept of collocation in control schemes, which refers to the placement of sensors and actuators in a way that they act on the same degree-of-freedom of the controlled structure. Although perfect collocation is not achievable, quasi-collocated couples can be achieved by placing sensors and actuators nearby. Collocated systems have advantages in terms of stability because the phase between a collocated pair actuator/sensor is contained in the range of 0 to -180 degrees in a large frequency bandwidth. However, it is not always possible to achieve collocation in practical applications, such as in robotic systems and acoustic ducts, where the error is measured far away from the source of the actuation [8].

The paragraph discusses the challenges associated with the control of multiple normal modes of vibrations in a structure using a Multiple Input - Multiple Output (MIMO) architecture. In a MIMO architecture, there are several actuators and sensors that need to be used to control different normal modes of vibrations. This requires defining a model for the coupled electromechanical response of the system. One approach to solving this problem is by using sensor and actuator participation matrices to relate the vector of sensor voltages and actuator voltages with the equations of motion of the structure [9]. Positive Position Feedback (PPF) is a feedback control algorithm that has been used successfully with PPF for a number of actuators and sensors equal to or smaller than the number of normal vibration modes under control [10]. PPF adds damping to the targeted resonant frequency by giving a signal in phase with velocity. PPF causes important vibration reductions and is easily tuned by empirical methods. However, MIMO PPF strategies require determining the sensor and actuator participation matrices that express the electromechanical coupling between the piezoelectric transducers and the vibrations of the structure. The determination of the electromechanical

coupling is based on analytical, finite-element, or reduced-order models of the controlled system.

In this paragraph, the authors discuss a method for determining the coupling matrices for a non-collocated control architecture with piezoelectric elements. They mention that the empirical determination of the coupling matrices for such systems has received little attention in the literature. The authors propose a new method based on modal analysis and experimental measurements. They used a commercial modal analysis suite to provide natural frequencies, mode shapes, damping ratios, and modal force for the first eleven modes of a sandwich plate with non-collocated piezoelectric patches. Then, they carried out a set of experimental measurements while exciting the structure solely through the actuator patches and recorded the piezoelectric signals from the sensors. Using experimental responses, the coupling matrices of sensors and actuators were determined through a method based on least square error minimization. The effectiveness of the proposed method was validated by comparing the experimentally observed vibrations with a numerical simulation, and then the PPF control of the first eight modes of the plate was implemented using the block-inverse technique. Good reductions of vibration amplitude were experimentally observed for all the eight modes, confirming the effectiveness of the proposed method in identifying the coupling matrices and developing an active vibration control. The authors suggest that this method could simplify considerably the implementation of active structures and their diffusion in engineering products, especially if coupled with an automated tuning of the PPF parameters during the operation of continuous structures.

2 METHODS

Continuous structures equipped with smart transducers are electromechanical systems with an infinite number of degrees of freedom (DOFs). After discretization, the number of DOFs is reduced to n. It is often counterproductive to actively control a large number of DOFs. Thus, Reduced Order Models (ROMs) are commonly built for the smart structures under consideration, independently on the strategy of active control. A system with n DOFs and m actuators is described by the equation of motion,

$$\boldsymbol{M}\ddot{\boldsymbol{x}} + \boldsymbol{C}\dot{\boldsymbol{x}} + \boldsymbol{K}\boldsymbol{x} = \boldsymbol{F} + \boldsymbol{B_a}\boldsymbol{V_a} \tag{1}$$

where the mass matrix $\boldsymbol{M}$, the damping matrix $\boldsymbol{C}$ and the stiffness matrix $\boldsymbol{K}$ have dimension [n x n]. $\boldsymbol{F}$ is the vector of the external forces (disturbances) [n x 1], $\boldsymbol{V_a}$ is the vector of the actuator voltages [m x 1] and $\boldsymbol{B_a}$ is the actuator participation matrix [n x m]. $\boldsymbol{x}$ is the vector of the system generalized coordinates [n x 1]. If the system is provided with sensors as well, their voltages $\boldsymbol{V_s}$ are described by the equation,

$$\boldsymbol{V_s} = \boldsymbol{C_s}\boldsymbol{x} \tag{2}$$

where $\boldsymbol{C_s}$ is the sensor participation matrix [m x n].

To simplify this problem, eq. (1) can be posed as an eigenvalue problem, and the corresponding $\boldsymbol{\Phi}$ (normalized eigenvector matrix of size [n x n]) and $\boldsymbol{\eta}$ (normal coordinates vector of size [n x 1]) can be found out such that $\boldsymbol{\Phi}^{\mathrm{T}}\boldsymbol{M}\boldsymbol{\Phi}$ is a diagonal unity matrix. If the

displacement $\boldsymbol{x}$ is dominated by k eigenvectors, the following approximation can be made using modal truncation,

$$\boldsymbol{x} \cong \boldsymbol{\Phi}'\boldsymbol{\eta}', \tag{3}$$

where, $\boldsymbol{\Phi}'[n \text{ x } k]$ and $\boldsymbol{\eta}'[k \text{ x } 1]$ are truncated eigenvector matrix and normal coordinates vector with $k < n$. In the following text, the prime notation is ignored, and only truncated eigenvector matrix and normal coordinates vector are used. Eq. (1) is pre-multiplied by the matrix of the eigenvectors $\boldsymbol{\Phi}^{\mathrm{T}}$ $[k \text{ x } n]$ and eqs. (1) and (2) are re-written considering the modal truncation eq. (3) to obtain the normalized modal equations,

$$\boldsymbol{I}\ddot{\boldsymbol{\eta}} + \boldsymbol{2}[\boldsymbol{\zeta_k}\boldsymbol{\omega_k}]\dot{\boldsymbol{\eta}} + [\boldsymbol{\omega_k^2}]\boldsymbol{\eta} = \overline{\boldsymbol{F}} + \overline{\boldsymbol{B_a}}\boldsymbol{V_a}, \tag{4}$$

$$\boldsymbol{V_s} = \overline{\boldsymbol{C_s}}\boldsymbol{\eta}, \tag{5}$$

where, $\overline{\boldsymbol{F}} = \boldsymbol{\Phi}^{\mathrm{T}}\boldsymbol{F}$, $\overline{\boldsymbol{B_a}} = \boldsymbol{\Phi}^{\mathrm{T}}\boldsymbol{B_a}$ and $\overline{\boldsymbol{C_s}} = \boldsymbol{C_s}\boldsymbol{\Phi}$, $[\boldsymbol{\zeta_k}\boldsymbol{\omega_k}] = \begin{bmatrix} 2\zeta_1\omega_1 & \cdots & 0 \\ \vdots & \ddots & \vdots \\ 0 & \cdots & 2\zeta_k\omega_k \end{bmatrix}$, and $[\boldsymbol{\omega_k^2}] = \begin{bmatrix} \omega_1^2 & \cdots & 0 \\ \vdots & \ddots & \vdots \\ 0 & \cdots & \omega_k^2 \end{bmatrix}$.

Any simulation of the active control relies on the knowledge of the matrices $\overline{\boldsymbol{B_a}}[k \text{ x } m]$ and $\overline{\boldsymbol{C_s}}$ $[m \text{ x } k]$. Several works in the literature [9], [11] make use of a preliminary construction of a finite-element model for the coupled structure. In this case, the matrices $\boldsymbol{M}$, $\boldsymbol{C}$, $\boldsymbol{K}$, $\boldsymbol{B_a}$, and $\boldsymbol{C_s}$, as well as the relationship between the voltages $\boldsymbol{V_s}$ and $\boldsymbol{V_a}$ with the displacements of the structure are known. Then, $\overline{\boldsymbol{B_a}}$ and $\overline{\boldsymbol{C_s}}$ are calculated as per the above equations.

In this paper, a method is proposed to obtain the electro-mechanical coupled equations (eqs. (4) and (5)) through simple experimental measurements only. The method assumes that the following measurements are possible for the structure. First, the structure must be subjected to a punctual pseudo-random excitation and the responses at the n coordinates associated to the n DOFs must be measured $\boldsymbol{x_E}$ without supplying voltage to the actuators. Here $\boldsymbol{x_E}$ is a function of time. However, it is convenient to work in the frequency domain by using the Frequency Response Functions (FRFs) describing the vibration responses of the n generalized coordinates with respect to the punctual pseudo-random excitation. Subsequently, the punctual excitation must be removed and each of the m actuators receive random signal voltages separately and the corresponding responses at the n generalized coordinates must be measured; the m vectors of dimension n, each one obtained actuating a single actuator, are $(\boldsymbol{x_1}, \boldsymbol{x_2}, \boldsymbol{x_3}, \ldots \boldsymbol{x_m})$. Also in this case, it is convenient to work in the frequency domain with FRFs. Similarly, the corresponding sensor voltages $\boldsymbol{V_{sE}}$, associated to $\boldsymbol{x_E}$, and $(\boldsymbol{V_{s1}}, \boldsymbol{V_{s2}}, \boldsymbol{V_{s3}}, \ldots, \boldsymbol{V_{sm}})$, associated to $(\boldsymbol{x_1}, \boldsymbol{x_2}, \boldsymbol{x_3}, \ldots \boldsymbol{x_m})$,must also be measured in each of these above-mentioned scenarios.

Modal analysis relies on the measurement of the external punctual force $\boldsymbol{F}$ and of the resulting displacements $\boldsymbol{x_E}$ to obtain the natural frequencies $\boldsymbol{\omega_k}$, damping ratios $\boldsymbol{\zeta_k}$ and normal modes $\boldsymbol{\Phi}$ of the system. Several validated modal parameter extraction algorithms are

available for this purpose. The case in which $\boldsymbol{V_a} = 0$ is called open-circuit case and eq. (4) takes the form

$$\boldsymbol{I\ddot{\eta} + 2[\zeta_k \omega_k]\dot{\eta} + [\omega_k^2]\eta = \bar{F}}. \tag{6}$$

Once $\boldsymbol{\Phi}$, $\boldsymbol{\omega_k}$ and $\boldsymbol{\zeta_k}$ are obtained from the modal analysis, the numerical model of the system under study can be built using eq. (6), without the electro-mechanical coupling term ($\overline{\boldsymbol{B_a}}$, $\overline{\boldsymbol{C_s}}$). For identifying $\overline{\boldsymbol{B_a}}$, a set of the m measurements ($\boldsymbol{x_1, x_2, x_3, \ldots x_m}$) is utilized. In these m measurements, the external punctual excitation is removed ($\boldsymbol{F} = 0$) and eq. (4) then takes the form

$$\boldsymbol{I\ddot{\eta} + 2[\zeta_k \omega_k]\dot{\eta} + [\omega_k^2]\eta = \overline{B_a} V_a}. \tag{7}$$

Considering a four-actuator case ($m = 4$), the $\overline{\boldsymbol{B_a}}$ matrix can be split into 4 subvectors as follows,

$$\overline{\boldsymbol{B_a}} = [\overline{\boldsymbol{B_{a1}}}, \overline{\boldsymbol{B_{a2}}}, \overline{\boldsymbol{B_{a3}}}, \overline{\boldsymbol{B_{a4}}}]. \tag{8}$$

When considering only the first actuator with voltage $\boldsymbol{V_a} = \{V_{a1}, 0, 0, 0\}^{\mathrm{T}}$ where V_{a1} is a random signal and expanding, eq. (7) takes the form,

$$\begin{bmatrix} 1 & \cdots & 0 \\ \vdots & \ddots & \vdots \\ 0 & \cdots & 1 \end{bmatrix} \ddot{\boldsymbol{\eta}} + \begin{bmatrix} 2\zeta_1\omega_1 & \cdots & 0 \\ \vdots & \ddots & \vdots \\ 0 & \cdots & 2\zeta_k\omega_k \end{bmatrix} \dot{\boldsymbol{\eta}} + \begin{bmatrix} \omega_1^2 & \cdots & 0 \\ \vdots & \ddots & \vdots \\ 0 & \cdots & \omega_k^2 \end{bmatrix} \boldsymbol{\eta} = V_{a1} \overline{\boldsymbol{B_{a1}}}. \tag{9}$$

Since the modal parameters $\boldsymbol{\omega_k}, \boldsymbol{\zeta_k}$, and $\boldsymbol{\phi}$ are available from the modal analysis, the vector $\overline{\boldsymbol{B_{a1}}}$ can be evaluated by means of a least-square method using eq. (9) transformed in the frequency domain.

The same procedure can be repeated for the other m-1 actuators by using the respective experimental responses ($\boldsymbol{x_2, x_3, x_4}$) in order to obtain the remaining $\overline{\boldsymbol{B_{a2}}}$, $\overline{\boldsymbol{B_{a3}}}$, $\overline{\boldsymbol{B_{a4}}}$. Subsequently, the matrix $\overline{\boldsymbol{C_s}}$ can be determined by means of a least-square approximation using eq. (5) and substituting $\boldsymbol{\eta = \Phi^{-1} x_E}$,

$$\boldsymbol{V_{sE} = \overline{C_s} \Phi^{-1} x_E}. \tag{10}$$

Similar to eq.(9), eq.(10) can be minimized in the frequency domain using FRFs instead of time responses. It must be noted that the eigenvectors provided by several modal analysis suites are already normalized with respect to mass, therefore the mass matrix $\boldsymbol{M}$ is not required.

In conclusion, $\overline{\boldsymbol{B_a}}$ and $\overline{\boldsymbol{C_s}}$ can be determined experimentally with relative ease. According to eqs. (7) and (10), $\overline{\boldsymbol{B_a}}$ allows the prediction of the modal response of the coupled structure to an imposed excitation voltage vector $\boldsymbol{V_a}$, while $\overline{\boldsymbol{C_s}}$ allow the prediction of the sensor voltage vector $\boldsymbol{V_s}$ corresponding to an imposed modal vibration $\boldsymbol{\eta}$.

In the case of the implementation a MIMO PPF algorithm to control the system under consideration, a coupled system of equations needs to be derived which relates the PPF coordinates Q to the modal coordinates. Here, if a number k of PPFs is introduced to control a number k of modes, the coupled system of equations is [9]

For implementing the MIMO PPF active vibration control through experiments, the actuator voltages $\boldsymbol{V_a}$ must be calculated from the sensor voltages $\boldsymbol{V_S}$ using the equations available in [9],

$$\boldsymbol{V_a}(s) = \boldsymbol{B_a^* G^{\frac{1}{2}}}\,[\boldsymbol{\omega_{fk}^4}]\widehat{\boldsymbol{H}}(\omega)\,\boldsymbol{G^{\frac{1}{2}} C_s^* V_S}(\omega), \tag{11}$$

where $\widehat{\boldsymbol{H}}(\omega) = \begin{bmatrix} \widehat{H}_1(\omega) & \cdots & 0 \\ \vdots & \ddots & \vdots \\ 0 & \cdots & \widehat{H}_k(\omega) \end{bmatrix}$,

and the transfer function of the each PPF is defined as follows.

$$\widehat{H}_k(\omega) = \frac{\mathbf{1}}{-\omega^2 + 2j\omega\boldsymbol{\zeta_{fk}}\boldsymbol{\omega_{fk}} + \boldsymbol{\omega_{fk}^2}}, \tag{12}$$

where the subscript k indicates the k-th PPF branch, and ω is the frequency. The output of the k-th PPF transfer function is a modal force with a phase of 180 degrees with respect to the modal force of external disturbance $\overline{\boldsymbol{F}}$. As a result, each PPF branch considerably dampens the vibration in correspondence of the specific generalized coordinate. Therefore, the PPF algorithm is modal in character, as its transfer function acts on generalized coordinates rather than on physical displacements.

3 EXPERIMENTAL SETUP

3.1 Sandwich Plate

The studied structure is a sandwich plate with dimensions of 900x460 mm and a thickness of 3.3 mm. It consists of a 2.62 mm foam core and four 0.17 mm thick unidirectional carbon fiber skins in a 0/90 configuration, bonded with epoxy glue. The plate is suspended by its corners from an aluminum frame with elastic cords and nylon strings to simulate free boundary conditions. Refer to Fig. 1 for visualization.

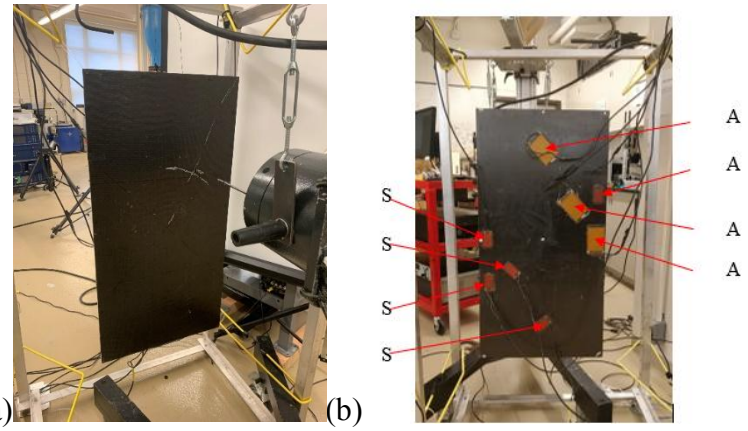

Figure. 1: a) Sandwich plate with boundary conditions. b) Sandwich plates equipped with piezoelectric sensors. Element S is the piezoelectric sensor. Element A is the piezoelectric actuator.

3.2 Piezoelectric Sensors and Actuators

The sandwich plate was suspended by its four corners from an aluminum frame using elastic cords and nylon strings, both under minimal tension to mimic free boundary conditions. Four DuraAct P-876.A15 piezoelectric patches were used as sensors, while three Macro Fiber Composite piezoelectric patches Model M-8557-P1, together with one P-876.A15, were used as actuators, powered by TREK High Voltage Power Amplifiers, model PA05039. Both transducers used employ Lead Zirconium Titanate (PZT) as the piezoelectric element and can be used as actuator or sensors interchangeably. The DuraAct and the Macro Fiber Composites act in bending only and their specifications are given in Table 1.

Table 1. Sensor and actuator specifications

Transducer	Height (mm)	Width (mm)	Capacitance (nF)	Voltage range (V)	Blocking force (N)	Strain (ppm)
MFC Actuator	85	57	16	-500-1500	693	1350
DuraAct Sensor	61	35	45	-250-1000	775	800

The piezoelectric sensors and actuators were positioned based on the maximum value of the modal strain energy of the first four modes of the free plate, modelled without the transducers. This setup was selected to match the one presented in [12], designed to control the first four modes of the structure.

3.3 Vibration measurement

The plate was excited via a Brüel & Kjaer Vibration Exciter type 4808 in direction orthogonal to the plate with a range of 5 Hz to 10 kHz at a point 95 mm right and 175 mm up from the center. The exciter was powered by a Brüel & Kjaer Power amplifier type 2718. A pseudo-random excitation was applied. The displacement and velocity of the vibrating plate was then measured using a Polytec PSV-500 Scanning Laser Head, controlled by the Polytec PSV-500 Vibrometer Front End. A diagram of the excitation and vibration measurement system is shown in Fig. 2(a). The Polytec Vibrometer front-end also generates the pseudo-random excitation signal that is fed into the power amplifier model 2718. The Polytec PSV-500 Scanning Laser Head has an accuracy of 60 nm and was selected for its scanning capabilities. A 7 x 13 points grid was used when scanning the plate. Nine extra points were also added, one at the center of each actuator and each sensor, as well as one at the position of the excitation. The final grid had a total of 98 active points. The main output of the scanning laser system was the experimental H1 frequency response function for each point on the grid.

3.4 Measurement of electromechanical coupling

The piezoelectric transducers were controlled by a dSpace DS1103 PPC Controller Board which also performed real-time data acquisition. Simulink models were loaded via the dSpace Control Desk software from a host PC. Charge amplifiers were not needed as the sensors provided sufficient signals and short cables reduced charge losses. The plate response $\boldsymbol{x_E}$ was

measured using the Polytec PSV-500 Scanning Laser Head while the sensors voltages $\boldsymbol{V_{sE}}$ were measured using the Polytec data acquisition system. To determine the electromechanical coupling, each actuator was used to excite the plate individually and a full scan of the plate's vibrations was performed for each case ($\boldsymbol{x_1}, \boldsymbol{x_2}, \boldsymbol{x_3}$ an $\boldsymbol{x_4}$). The shaker was disconnected during the actuator measurements to avoid altering the boundary conditions of the plate. The vibration scans were performed using the same grid shown in Fig. 2(b), and the same frequency range of DC to 200 Hz.

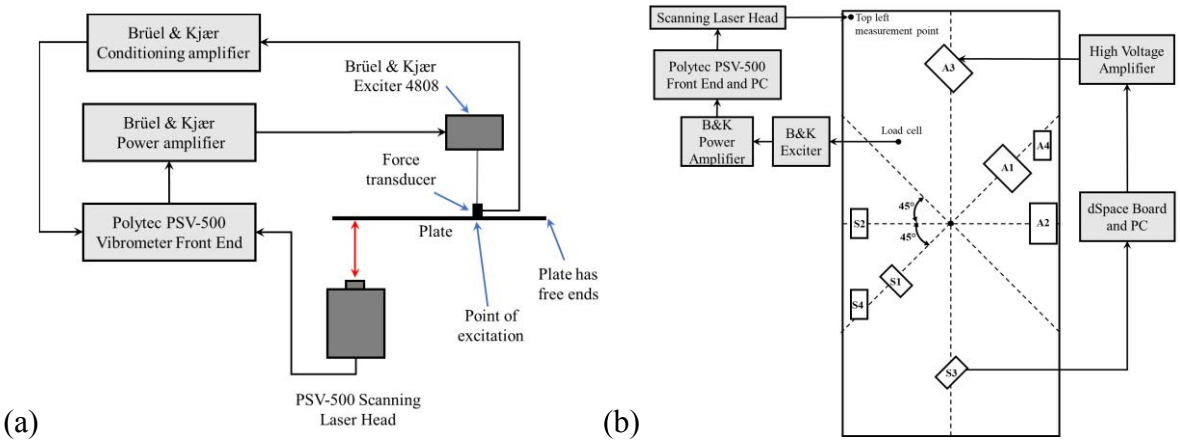

Figure. 2: a) Diagram of the excitation and measurement systems. b) Diagram of experimental setup with actuators and sensors. Actuators are labelled with the letter A, and sensors are labelled with S.

4 RESULTS

4.1 Experimental Modal Analysis

Experimental mo al analysis was con uc te on the plate's response x_E using the industry leading Siemens LMS PolyMAX modal parameter estimation algorithm [13]. The resulting natural frequencies and modal damping ratios are presented in Table 2 for the first 11 frequencies.

4.2 Participation matrices

In the coupled case under study, = 4 actuators and 4 sensors are used for the control of k = 8 normal modes of vibration by means of k = 8 PPF filters in the feedback loop. As a consequence, the actuator participation matrix based on the modal coordinates $\overline{\boldsymbol{B_a}}$ and the sensor participation matrix based on the modal coordinates $\overline{\boldsymbol{C_s}}$ have dimensions 8x4 and 4x8 respectively. The pseudo-inverse matrices base on Kwak's block-inverse technique, $\boldsymbol{B_a}^*$ for actuators and $\boldsymbol{C_s}^*$ for sensors, are 4x8 and 8x4, respectively. Smaller singular values are cut-off below certain values to ensure that very small values (corresponding to a minor influence

on that mode from a specific actuator) in the $\overline{\boldsymbol{B_a}}$ does not explode during the inversion process.

The fitness of the matrix $\overline{\boldsymbol{B_a}}$ is first validated by fitting the experimental uncontrolled response of the plate ($\boldsymbol{x_1, x_2, x_3, x_4}$) with the uncontrolled response of numerical simulation according to eq. (9), as described in the Methods section. The comparison at the top left point of the sandwich plate for the case of actuators 1 is shown in Fig. 3 (a). Both the real and imaginary part of the responses were compared and found to be in very good agreement. However, for the sake of simplicity, only the amplitude response is presented in Fig. 3 (a).

Table 2. Experimental natural frequencies and modal damping of the first 11 modes of plate with actuators and sensors.

Mode #	Natural Frequency (Hz) - Numerical	Natural Frequency (Hz) - Experimental	Modal Damping (%)
1	18.424	20.325	3.14
2	30.107	30.847	0.67
3	48.484	47.476	1.28
4	81.144	81.931	1.28
5	96.610	94.120	1.32
6	124.86	99.602	0.89
7	129.41	106.252	0.69
8	145.21	121.883	0.54
9	154.17	153.869	1.04
10	167.00	160.179	1.13
11	178.32	172.011	0.62

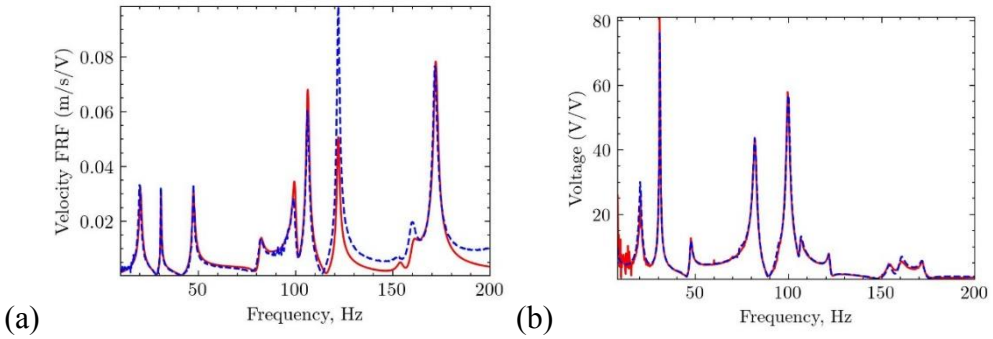

Figure. 2: Comparison at the top left point of the sandwich plate of the experimentally measured data (continuous line) and the numerical results (dashed line) with the identified $\overline{\boldsymbol{B_a}}$ and $\overline{\boldsymbol{C_s}}$ matrix: (a) Actuator 1, (b) Sensor 1.

Similarly, the validation of the $\overline{\boldsymbol{C_s}}$ matrix was carried out by comparing the experimentally measured sensor voltage $\boldsymbol{V_{sE}}$ with the numerical results from the sandwich plate response $\boldsymbol{x_E}$. A very good agreement between the experimental and numerical sensor response was observed and it is shown in Fig. 3 (b).

4.3 Active vibration control (AVC)

The performance of the actuator, $\boldsymbol{B_a^*}$, and sensor, $\boldsymbol{C_s^*}$, participation matrices is also evaluated by applying a MIMO PPF active control strategy for the vibration mitigation of 8 normal modes of vibration through 8 PPF low-pass filters in the control loop. The Simulink diagram describing the control algorithm is shown in Fig. 4. The parameters in the PPF transfer functions were tuned according to the procedure described in the Methods section; thus, the resonant frequency $\boldsymbol{\omega_{fk}}$ of each PPF was made equal to one resonant frequency of the plate $\boldsymbol{\omega_k}$; the damping parameter of each PPF controller was fixed at the value $\boldsymbol{\zeta_{fk}} = 0.3$. The eight multiplicative gains $\boldsymbol{g_k}$ required by the eight controllers were found empirically by taking into consideration each resonance of the plate sequentially, starting from the highest frequency. At each frequency, the highest gain value not causing instability was chosen; see Table 3.

Table 3. Gains applied to the transfer functions of the PPF controllers.

g_1	g_2	g_3	g_4	g_5	g_6	g_7	g_8
0.65	0.5	0.025	0.02	0.06	0.02	0.025	0.05

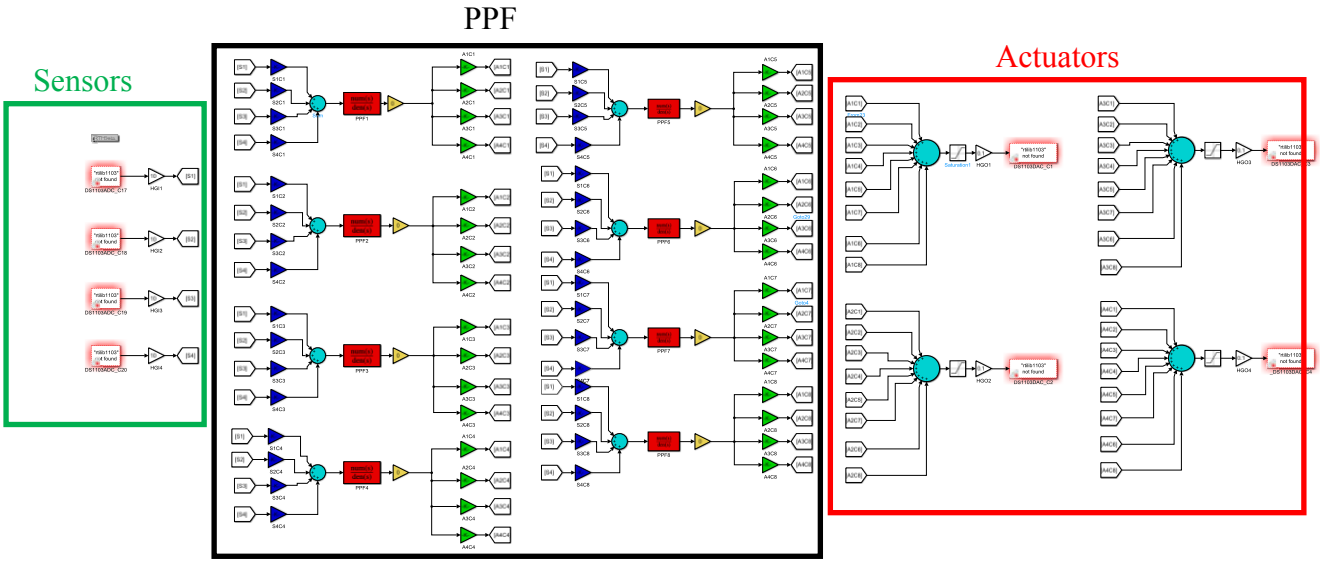

Figure 4: Simulink chart of the active control algorithm. Blue blocks: scalar gains corresponding to the elements in the matrix $\boldsymbol{B_a}^*$; red blocks: transfer functions of the PPF filters; yellow blocks: scalar gains g_i applied to the PPF transfer functions; green blocks: scalar gains corresponding to the elements in the matrix $\boldsymbol{C_s}^*$; cyan blocks: summations; white triangles: hardware gains; white pentagons: callbacks; white squares: saturations; rectangles with red halo: transducers.

The resulting control dampens effectively the first eight modes of the plate when these are excited by a pseudo-random force applied by the shaker. The comparison of the experimental

uncontrolled and controlled vibration response at the top left corner of the plate is shown in Fig. 5(a). In addition to the experimental comparison, by means of the identified actuator and sensor matrices, the controlled response of the plate can also be simulated numerically, and the result is shown in Fig. 5(b). The numerical controlled responses match satisfactorily with the experimental ones. The vibration reduction achieved for the eight modes are -11, -24, -14, -7, -13, -20, -7 and -8 dB, respectively. The average reduction in all the modes combined is around 50% and -14 dB. The three higher modes (modes 9^{th} to 11^{th}) in Fig. 5(a) are practically unaffected by the AVC. Higher vibration reduction can be achieved by reposing the problem in such a way that $k = m$ (one actuator-sensor pair for one mode). Here, $k = 2m$ was chosen to demonstrate the usefulness of the presented method for the cases beyond $k = m$.

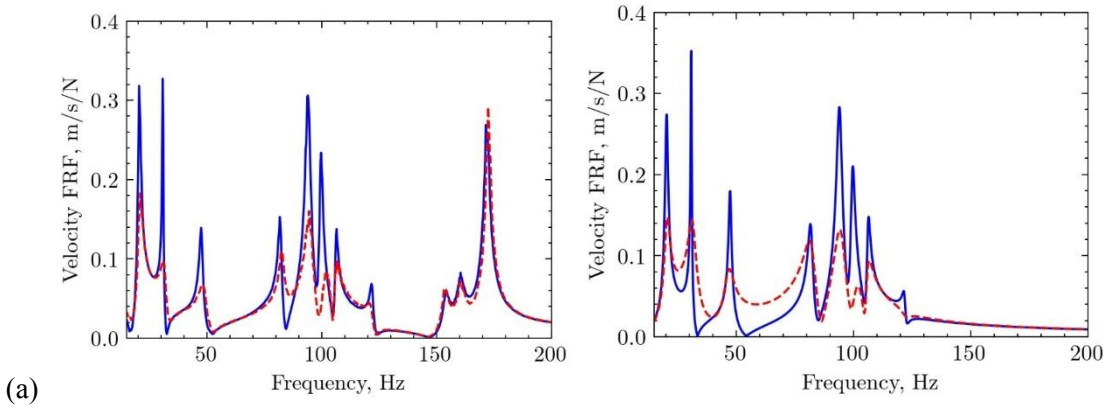

(a)

Figure 5: Comparison of controlled (dashed line) and uncontrolled (continuous line) response measured at the top left corner of the plate. (a) Experimental comparison (b) Numerical comparison.

As the numerical model accurately captures the response of the plate, more sophisticated optimization algorithms can be deployed to find better MIMO PPF parameters (i.e., those giving better vibration reduction) compared to the results of the block inversion technique. This is left for future study.

5 CONCLUSIONS

A new method was introduced for identifying the coupling matrices of a structure equipped with piezoelectric patches. The method was demonstrated on a sandwich plate and a MIMO PPF controller was developed based on the extracted coupling matrices. Vibration reduction on the first eight modes of the plate was achieved using only four non-collocated actuator-sensor pairs. The proposed method only requires an experimental apparatus capable of estimating the resonant frequencies, damping ratios, and mass-normalized normal modes of vibration of the smart structure under test, eliminating the need for a preliminary model. The method's applicability to more complex structures is left for future studies.

REFERENCES

[1] M. Amabili, *Nonlinear vibrations and stability of shells and plates*. Cambridge University Press, 2008.

[2] S. Carra, M. Amabili, R. Ohayon, and P.-M. Hutin, "Active vibration control of a thin rectangular plate in air or in contact with water in presence of tonal primary ist urbance," *Aerosp. Sci. Technol.*, vol. 12, no. 1, pp. 54–61, 2008.

[3] S. Carra, M. Amabili, an R. Ohayon, "Broa ba n active vibration control of a rectangular flexible wall of an empty and a water-fille tank," *J. Intell. Mater. Syst. Struct.*, vol. 18, no. 7, pp. 637–651, 2007.

[4] M. K. Kwak, *Dynamic modeling and active vibration control of structures*. Springer, 2022.

[5] T. Bailey an J. E. Ubbar , "Distribute piezoelectric-polymer active vibration control of a cantilever beam," *J. Guid. Control. Dyn.*, vol. 8, no. 5, pp. 605–611, 1985, doi: 10.2514/3.20029.

[6] H. S. Tzou an C. I. Tseng, "Distribute piezoelectric sensor/actuator e sign for dynamic measurement/control of distributed parameter systems: a piezoelectric finite element approach," *J. Sound Vib.*, vol. 138, no. 1, pp. 17–34, 1990.

[7] A. Donoso and J. C. Bellido, "Systematic e sign of ist ribute piezoelectric mo al sensors/actuators for rectangular plates by optimizing the polarization profile," *Struct. Multidiscip. Optim.*, vol. 38, no. 4, pp. 347–356, 2009.

[8] J.-H. Ryu, D.-S. Kwon, an B. Hannafor , "Control of a flexible manipulator with noncollocated feedback: time- omain passivity approach," *IEEE Trans. Robot.*, vol. 20, no. 4, pp. 776–780, 2004.

[9] M. K. Kwak an S. Heo, "Active vibration control of smart gri structure by multiinput and multioutput positive position fee ba ck controller," *J. Sound Vib.*, vol. 304, no. 1–2, pp. 230–245, 2007, doi: 10.1016/j.jsv.2007.02.021.

[10] J. L. Fanson an T. K. Caughey, "Positive position fee ba ck control for large space structures," *AIAA J.*, vol. 28, no. 4, pp. 717–724, 1990.

[11] K. M. Liew, X. Q. He, T. Y. Ng, an S. Kitipornchai, "Active control of FGM shells subjecte to a temperature gra ient via piezoelectric sensor/actuator patches," *Int. J. Numer. Methods Eng.*, vol. 55, no. 6, pp. 653–668, 2002.

[12] G. Ferrari an M. Amabili, "Active vibration control of a san wic h plate by non-collocate positive position fee ba ck," *J. Sound Vib.*, vol. 342, pp. 44–56, 2015, doi: 10.1016/j.jsv.2014.12.019.

[13] B. Peeters, H. Van e r Auweraer, P. Guillaume, an J. Leuri an, "The PolyMAX frequency- omain metho : a new stan a r for mo al parameter estimation?," *Shock Vib.*, vol. 11, no. 3–4, pp. 395–409, 2004.